Dissociative production of vector mesons as a new tool to study gluon saturation at electron-ion colliders [1]

Dagmar Bendová
in collaboration with J. Cepila and J. G. Contreras

Faculty of Nuclear Sciences and Physical Engineering
Czech Technical University in Prague

EPS HEP 2019, Ghent Belgium

13^{th} July, 2019

[1] Based on: DB , J. Cepila, J. G. Contreras, Phys. Rev. D 99, 034025 (2019)

Motivation: Gluon saturation

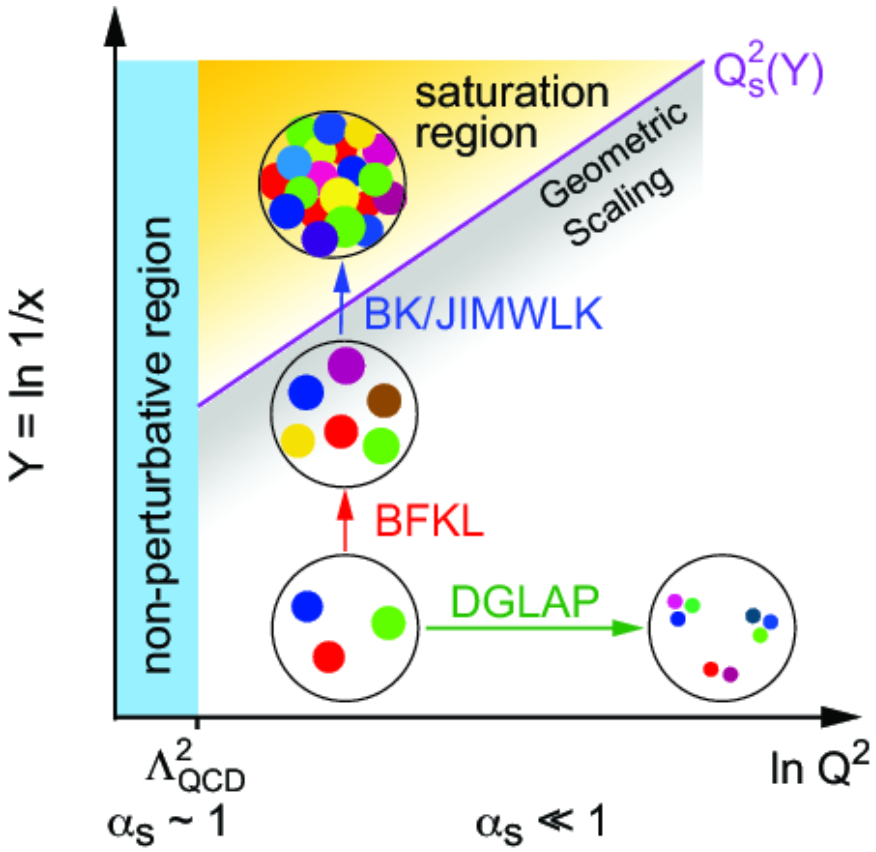

Figure: Diagram picturing the QCD evolution of the partonic structure of the proton.

C. Marquet, Nucl.Phys. A904-905 (2013) 294c-301c.

- Evolution of parton densities with increasing energy.

Motivation: Gluon saturation

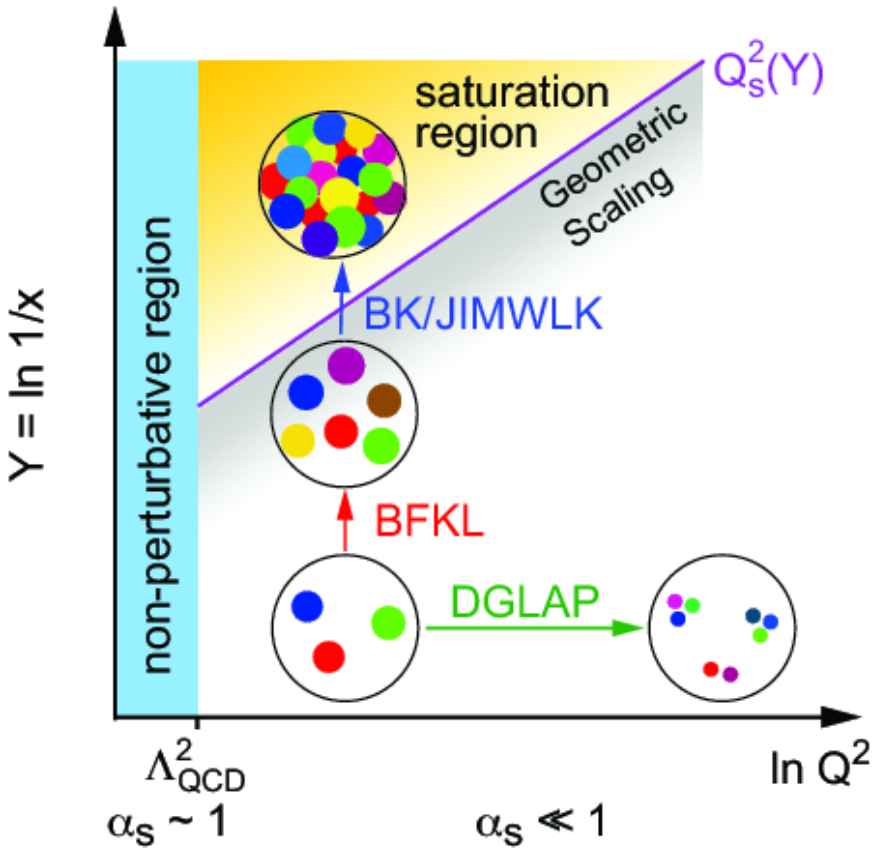

Figure: Diagram picturing the QCD evolution of the partonic structure of the proton.

C. Marquet, Nucl.Phys. A904-905 (2013) 294c-301c.

- Evolution of parton densities with increasing energy.
- By fixing the scale of the process, one can fix the position in ln Q^2.

Motivation: Gluon saturation

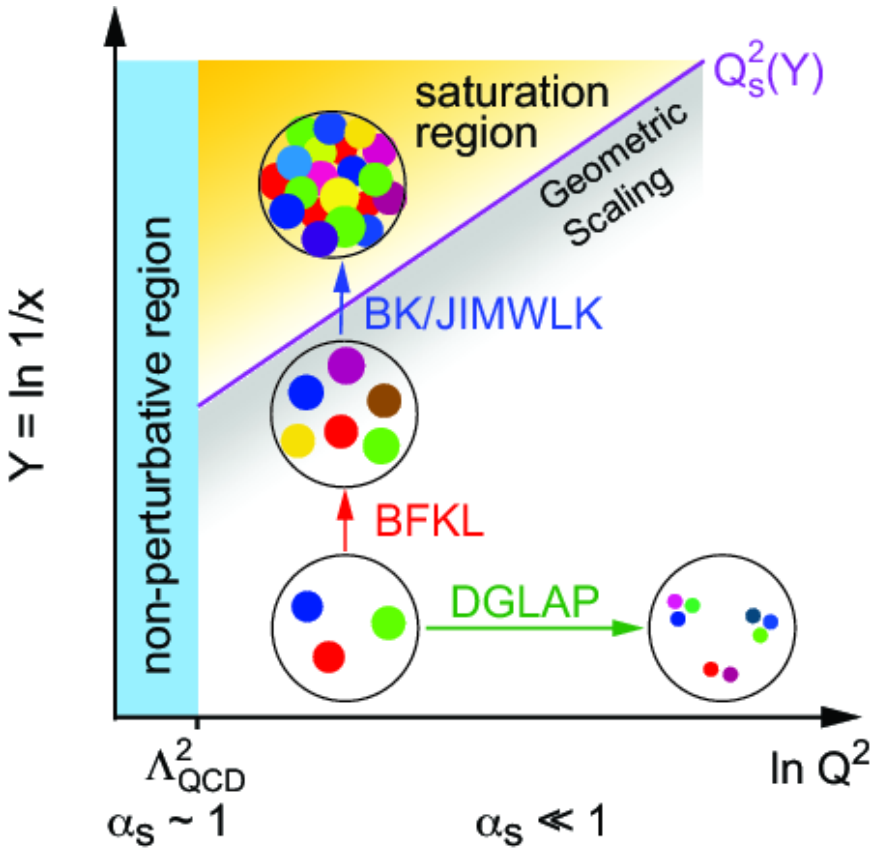

Figure: Diagram picturing the QCD evolution of the partonic structure of the proton.

C. Marquet, Nucl.Phys. A904-905 (2013) 294c-301c.

- Evolution of parton densities with increasing energy.
- By fixing the scale of the process, one can fix the position in ln Q^2.
- Going to smaller x, one can reach the saturation scale $Q_S^2(x)$
  - Below $Q_S^2(x) \rightarrow$ dilute regime, linear evolution of the gluon density (BFKL).
  - Above $Q_S^2(x) \rightarrow$ dense regime, non-linear evolution of the gluon density (JIMWLK, BK).

Motivation: Gluon saturation

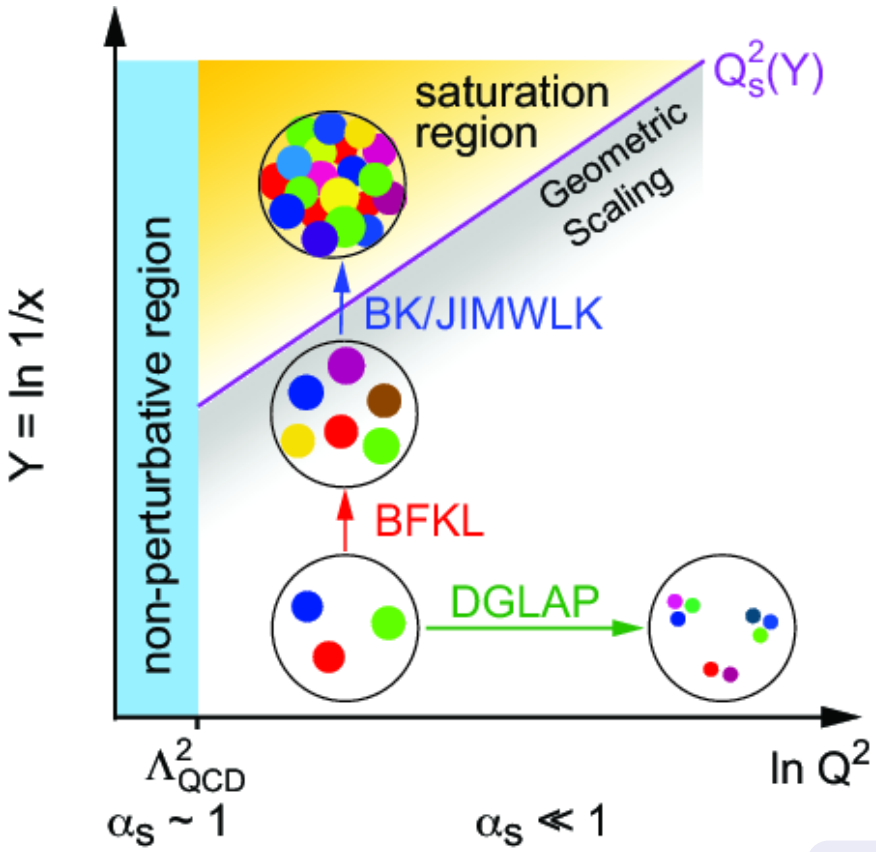

Figure: Diagram picturing the QCD evolution of the partonic structure of the proton.

C. Marquet, Nucl.Phys. A904-905 (2013) 294c-301c.

- Evolution of parton densities with increasing energy.
- By fixing the scale of the process, one can fix the position in ln Q^2.
- Going to smaller x, one can reach the saturation scale $Q_S^2(x)$
  - Below $Q_S^2(x) \rightarrow$ dilute regime, linear evolution of the gluon density (BFKL).
  - Above $Q_S^2(x) \rightarrow$ dense regime, non-linear evolution of the gluon density (JIMWLK, BK).

We include geometrical fluctuations of the proton structure and probe the saturation signal in dependence on the scale of the process.

What process is sensitive to the proton structure?

- We want to probe partonic structure of hadrons.
- Direct access to kinematics (x, Q^2).
- Easily observable final state is desirable.

What process is sensitive to the proton structure?

- We want to probe partonic structure of hadrons.
- Direct access to kinematics (x, Q^2).
- Easily observable final state is desirable.
- Exclusive and dissociative vector meson (VM) production fulfil both requirements.

$$Q^2 = -q^2 = -(k - k')^2$$

$$W^2_{\gamma p} = (p + q)^2$$

$$\Delta^2 = -t = -(p - p')^2$$

$$x = \frac{M^2 + Q^2}{W^2_{\gamma p} + Q^2}$$

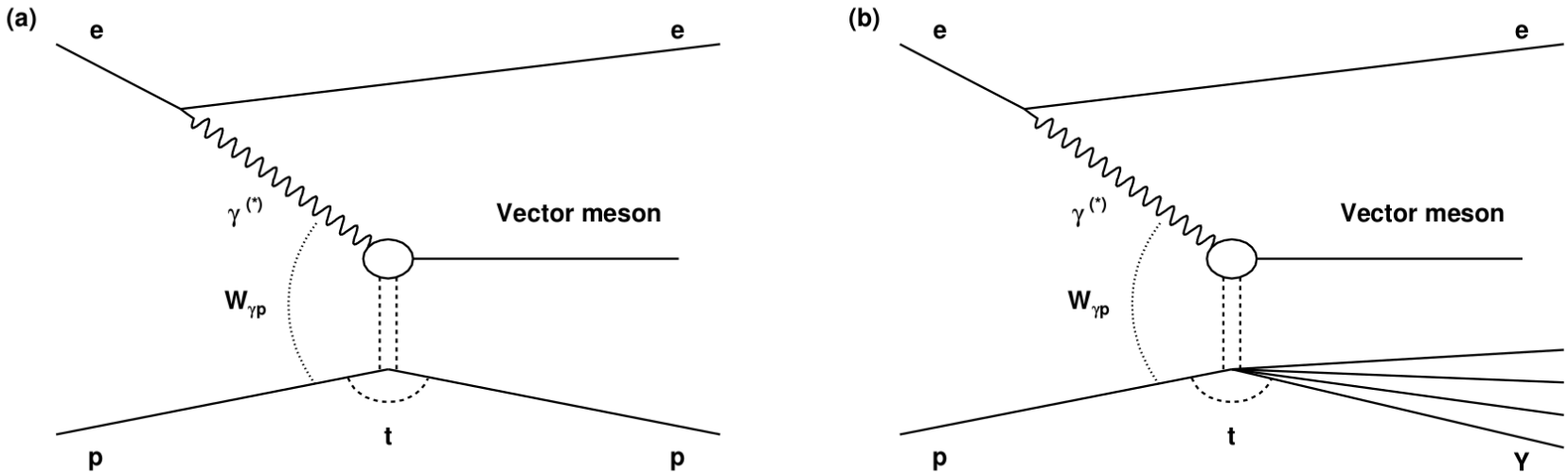

Figure: Diagrams for exclusive (a) and dissociative (b) production of vector mesons.

Scattering amplitude and the cross section

- Production of a vector meson can be calculated within the color dipole picture.
- The photon interacts via its $q\bar{q}$ Fock state with the proton in the target rest frame.

Scattering amplitude and the cross section

- Production of a vector meson can be calculated within the color dipole picture.
- The photon interacts via its $q\bar{q}$ Fock state with the proton in the target rest frame.
- The scattering amplitude is given as a convolution of the photon-VM wave function with the dipole cross section:

$$\mathcal{A}_{T,L}(x, Q^2, \vec{\Delta}) = i \int \mathrm{d}\vec{r} \int_0^1 \frac{\mathrm{d}z}{4\pi} \int \mathrm{d}\vec{b} |\Psi^*_{VM}\Psi_{\gamma^*}|_{T,L} \exp\left[-i\left(\vec{b} - (1-z)\vec{r}\right)\vec{\Delta}\right] \frac{\mathrm{d}\sigma_{q\bar{q}}}{\mathrm{d}\vec{b}}.$$

Scattering amplitude and the cross section

- Production of a vector meson can be calculated within the color dipole picture.
- The photon interacts via its $q\bar{q}$ Fock state with the proton in the target rest frame.
- The scattering amplitude is given as a convolution of the photon-VM wave function with the dipole cross section:

$$\mathcal{A}_{T,L}(x, Q^2, \vec{\Delta}) = i \int \mathrm{d}\vec{r} \int_0^1 \frac{\mathrm{d}z}{4\pi} \int \mathrm{d}\vec{b} |\Psi^*_{VM}\Psi_{\gamma^*}|_{T,L} \exp\left[-i\left(\vec{b} - (1-z)\vec{r}\right)\vec{\Delta}\right] \frac{\mathrm{d}\sigma_{q\bar{q}}}{\mathrm{d}\vec{b}}.$$

- Exclusive cross section to produce the vector meson

$$\left.\frac{\mathrm{d}\sigma^{\gamma^* p \to VMp}}{\mathrm{d}|t|}\right|_{T,L} = \frac{\left(R_g^{T,L}\right)^2}{16\pi} |\langle \mathcal{A}_{T,L}^{\gamma^* p \to VMp} \rangle|^2.$$

Scattering amplitude and the cross section

- Production of a vector meson can be calculated within the color dipole picture.
- The photon interacts via its $q\bar{q}$ Fock state with the proton in the target rest frame.
- The scattering amplitude is given as a convolution of the photon-VM wave function with the dipole cross section:

$$\mathcal{A}_{T,L}(x, Q^2, \vec{\Delta}) = i \int \mathrm{d}\vec{r} \int_0^1 \frac{\mathrm{d}z}{4\pi} \int \mathrm{d}\vec{b} |\Psi^*_{VM}\Psi_{\gamma^*}|_{T,L} \exp\left[-i\left(\vec{b} - (1-z)\vec{r}\right)\vec{\Delta}\right] \frac{\mathrm{d}\sigma_{q\bar{q}}}{\mathrm{d}\vec{b}}.$$

- Exclusive cross section to produce the vector meson

$$\left.\frac{\mathrm{d}\sigma^{\gamma^* p \to VMp}}{\mathrm{d}|t|}\right|_{T,L} = \frac{\left(R_g^{T,L}\right)^2}{16\pi} |\langle \mathcal{A}_{T,L}^{\gamma^* p \to VMp} \rangle|^2.$$

- Dissociative cross section is given as the variance over different configurations

$$\left.\frac{\mathrm{d}\sigma^{\gamma^* p \to VMY}}{\mathrm{d}|t|}\right|_{T,L} = \frac{\left(R_g^{T,L}\right)^2}{16\pi} \left(\langle |\mathcal{A}_{T,L}^{\gamma^* p \to VMp}|^2 \rangle - |\langle \mathcal{A}_{T,L}^{\gamma^* p \to VMp} \rangle|^2\right).$$

Scattering amplitude and the cross section

- Production of a vector meson can be calculated within the color dipole picture.
- The photon interacts via its $q\bar{q}$ Fock state with the proton in the target rest frame.
- The scattering amplitude is given as a convolution of the photon-VM wave function with the dipole cross section:

$$\mathcal{A}_{T,L}(x, Q^2, \vec{\Delta}) = i \int \mathrm{d}\vec{r} \int_0^1 \frac{\mathrm{d}z}{4\pi} \int \mathrm{d}\vec{b} |\Psi^*_{VM}\Psi_{\gamma^*}|_{T,L} \exp\left[-i\left(\vec{b} - (1-z)\vec{r}\right)\vec{\Delta}\right] \frac{\mathrm{d}\sigma_{q\bar{q}}}{\mathrm{d}\vec{b}}$$

- Exclusive cross section to produce the vector meson

$$\left.\frac{\mathrm{d}\sigma^{\gamma^* p \to VMp}}{\mathrm{d}|t|}\right|_{T,L} = \frac{\left(R_g^{T,L}\right)^2}{16\pi} |\langle \mathcal{A}_{T,L}^{\gamma^* p \to VMp} \rangle|^2.$$

- Dissociative cross section is given as the variance over different configurations

$$\left.\frac{\mathrm{d}\sigma^{\gamma^* p \to VMY}}{\mathrm{d}|t|}\right|_{T,L} = \frac{\left(R_g^{T,L}\right)^2}{16\pi} \left(\langle |\mathcal{A}_{T,L}^{\gamma^* p \to VMp}|^2 \rangle - |\langle \mathcal{A}_{T,L}^{\gamma^* p \to VMp} \rangle|^2\right).$$

Dipole-target cross section within the energy-dependent hot-spot model

- The differential dipole-proton cross section

$$\frac{\mathrm{d}\sigma_{q\bar{q}}}{\mathrm{d}\vec{b}} = 2N(x,\vec{r},\vec{b}) \rightarrow \sigma_0 N(x,\vec{r})\, T_p(\vec{b}).$$

- $T_p(\vec{b})$ describes the proton profile in the impact-parameter plane
- Normalization parameter σ_0 fixed as $\sigma_0 = 4\pi B_p$ with $B_p = 4.7\ \mathrm{GeV}^{-2}$.

[2] K. Golec-Biernat and M. Wusthoff, Phys. Rev. D 59 (1998) 014017.

Dipole-target cross section within the energy-dependent hot-spot model

- The differential dipole-proton cross section

$$\frac{\mathrm{d}\sigma_{q\bar{q}}}{\mathrm{d}\vec{b}} = 2N(x,\vec{r},\vec{b}) \to \sigma_0 N(x,\vec{r})\, T_p(\vec{b}).$$

- $T_p(\vec{b})$ describes the proton profile in the impact-parameter plane
- Normalization parameter σ_0 fixed as $\sigma_0 = 4\pi B_p$ with $B_p = 4.7\ \mathrm{GeV}^{-2}$.
- Dipole amplitude $N(x,\vec{r})$ can be obtained as a solution of BK equation or from various parametrizations.
  - **GBW parametrization**[2]

$$N(x,\vec{r}) = 1 - \exp\left(-\frac{\vec{r}^2 Q_s^2(x)}{4}\right)$$

    where $Q_s(x)$ denotes the x-dependent saturation scale

$$Q_s^2(x) = Q_0^2 \left(\frac{x_0}{x}\right)^{\lambda_{\mathrm{GBW}}}\ [\mathrm{GeV}^2].$$

  - We set $x_0 = 2 \cdot 10^{-4}$, $\lambda = 0.21$ and $Q_0^2 = 1\ \mathrm{GeV}^2$.

[2] K. Golec-Biernat and M. Wusthoff, Phys. Rev. D 59 (1998) 014017.

Proton profile in the impact-parameter plane

- We describe the proton profile using the **energy-dependent hot-spot model**[3].
  - Proton profile seen as a set of regions of high gluon density (hot spots) randomly placed in the impact parameter plane

$$T_p(\vec{b}) = \frac{1}{N_{hs}} \sum_{i=1}^{N_{hs}} T_{hs}\left(\vec{b} - \vec{b}_i\right).$$

[3] J. Cepila, J. G. Contreras and J. D. Tapia Takaki, Phys.Lett. B766 (2017) 186-191

Proton profile in the impact-parameter plane

- We describe the proton profile using the **energy-dependent hot-spot model**[3].
  - Proton profile seen as a set of regions of high gluon density (hot spots) randomly placed in the impact parameter plane

$$T_p(\vec{b}) = \frac{1}{N_{hs}} \sum_{i=1}^{N_{hs}} T_{hs}\left(\vec{b} - \vec{b}_i\right).$$

  - Each hot spot has a Gaussian distribution

$$T_{hs}(\vec{b}) = \frac{1}{2\pi B_{hs}} \exp\left(-\frac{\vec{b}^2}{2B_{hs}}\right), \quad B_{hs} = 0.8\ \mathrm{GeV}^{-2}.$$

  - The positions of the hot spots in the transverse plane fluctuate event-by-event.

[3] J. Cepila, J. G. Contreras and J. D. Tapia Takaki, Phys.Lett. B766 (2017) 186-191

Proton profile in the impact-parameter plane

- We describe the proton profile using the **energy-dependent hot-spot model**[3].
  - Proton profile seen as a set of regions of high gluon density (hot spots) randomly placed in the impact parameter plane

$$T_p(\vec{b}) = \frac{1}{N_{hs}} \sum_{i=1}^{N_{hs}} T_{hs}\left(\vec{b} - \vec{b}_i\right).$$

  - Each hot spot has a Gaussian distribution

$$T_{hs}(\vec{b}) = \frac{1}{2\pi B_{hs}} \exp\left(-\frac{\vec{b}^2}{2B_{hs}}\right), \quad B_{hs} = 0.8\ \mathrm{GeV}^{-2}.$$

  - The positions of the hot spots in the transverse plane fluctuate event-by-event.
  - **Number of hot spots depends on** x **as** (grows with decreasing x)

$$N_{hs} = p_0 x^{p_1}\left(1 + p_2\sqrt{x}\right)$$

$$p_0 = 0.011, \quad p_1 = -0.58, \quad p_2 = 300.$$

  - Final N_{hs} is obtained using the Zero-truncated Poisson distribution.

[3] J. Cepila, J. G. Contreras and J. D. Tapia Takaki, Phys.Lett. B766 (2017) 186-191

Examples of proton profiles

x = 2e-04 N_{hs} = 5

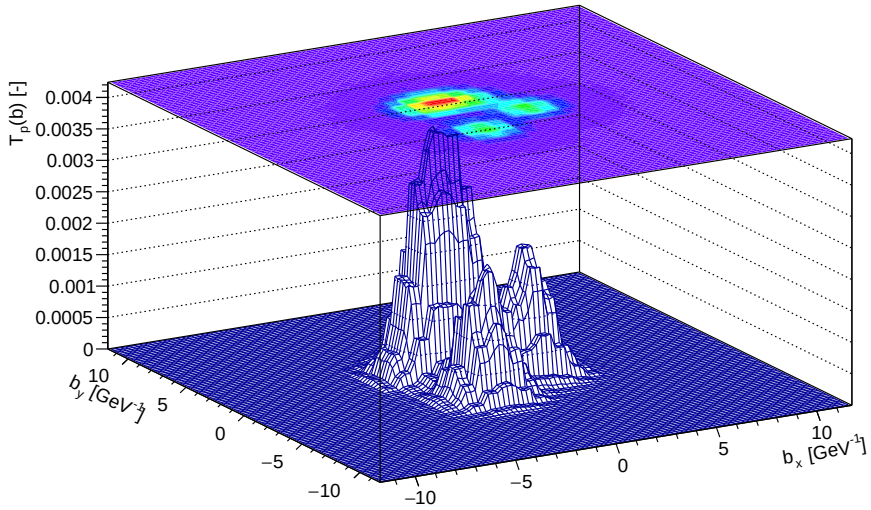

x = 1e-05 N_{hs} = 14

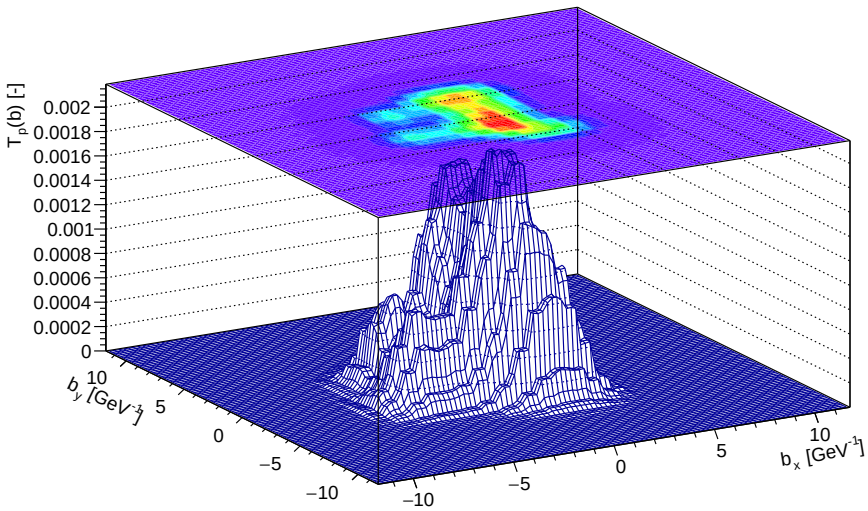

x = 1e-06 N_{hs} = 39

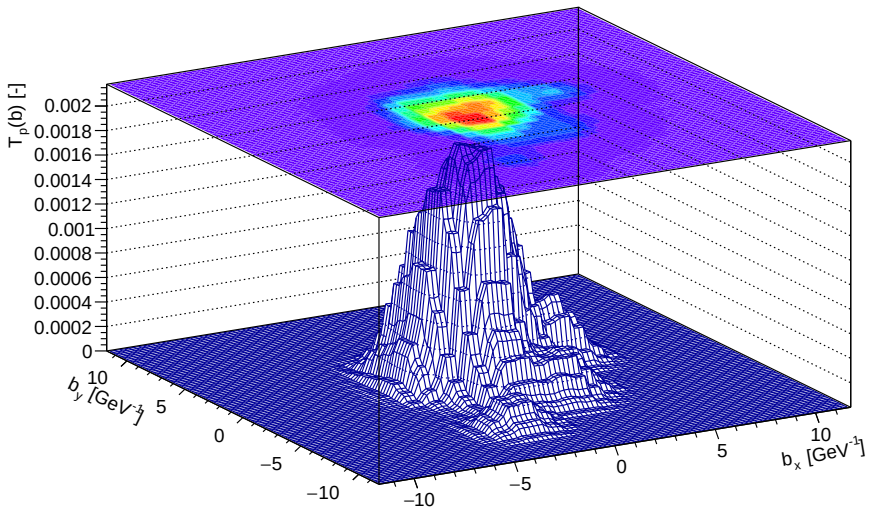

Predictions and comparison with data for cross sections of J/ψ meson

- Predictions compared to H1 and ALICE p–Pb data.
- Good agreement with the data.
- Dissociative maximum is clearly visible at all Q^2.

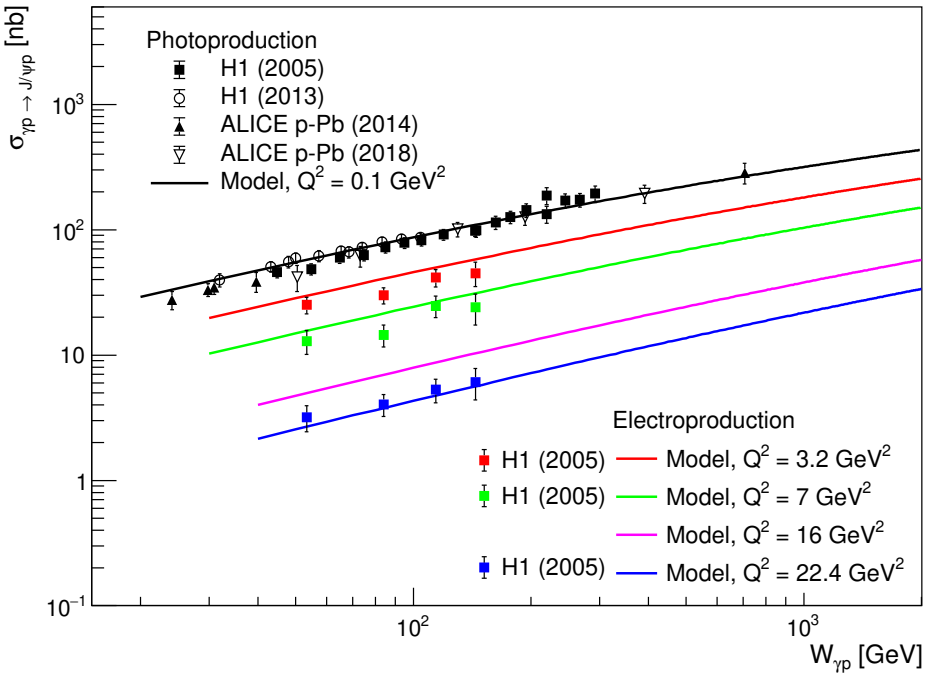

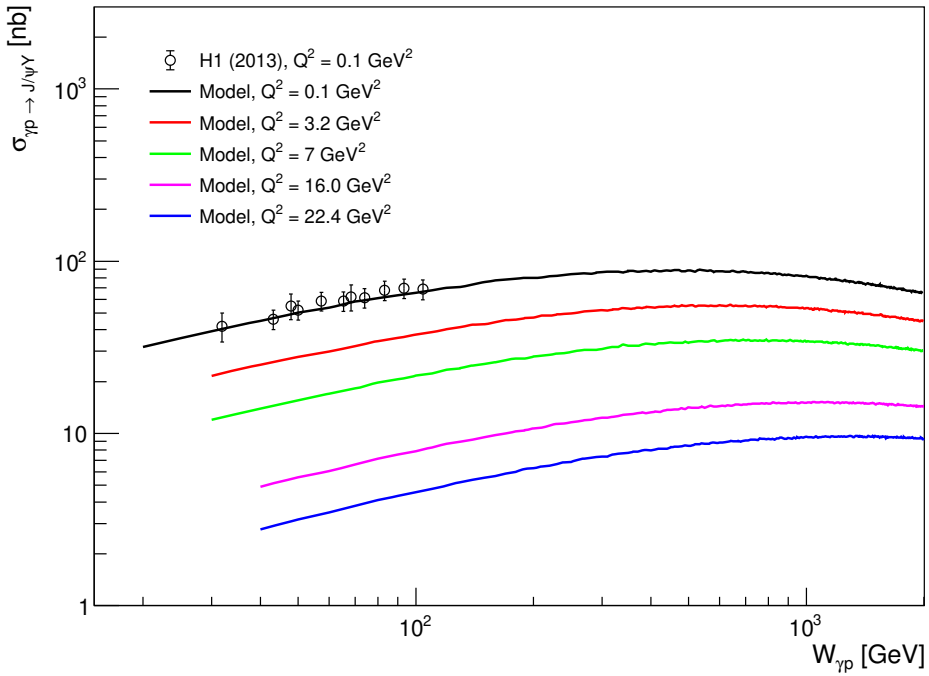

Predictions and comparison with data for cross sections of ρ meson

- Predictions compared to H1, ZEUS and preliminary CMS p–Pb data.
- Very good decription of electroproduction data for scales from $Q^2 = 2.4\ \mathrm{GeV}^2$ up to $Q^2 = 35.6\ \mathrm{GeV}^2$.
- For photoproduction B_p was changed[4] to $B_p = 8\ \mathrm{GeV}^{-2}$ in accordance with H1 measurements of the slope parameter b.[5]

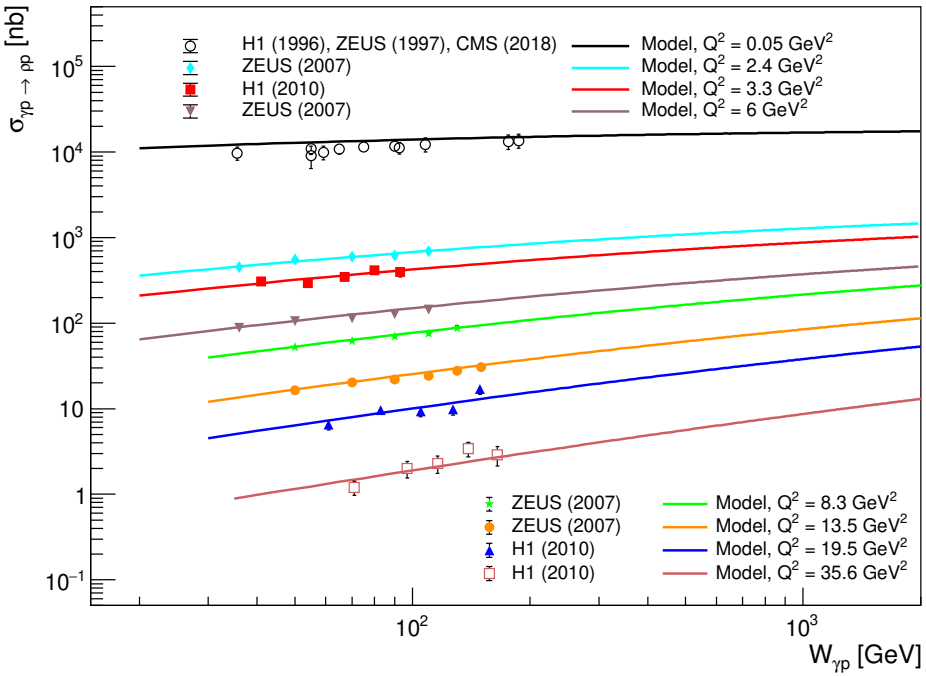

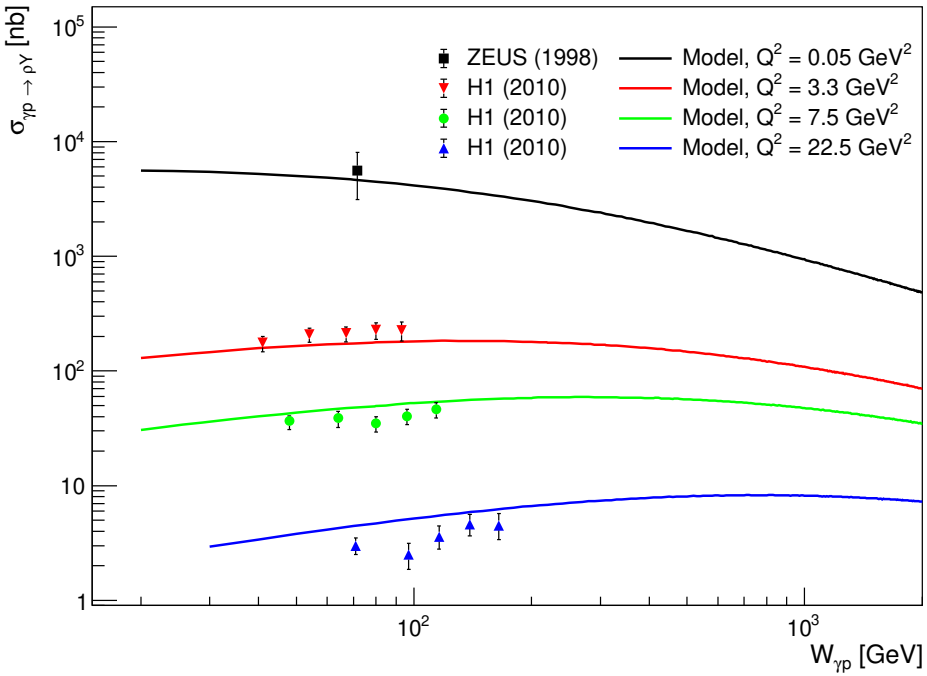

[4] J. Cepila, J. G. Contreras, M. Krelina and J. D. Tapia Takaki, Nucl.Phys. B934 (2018) 330-340

[5] H1 Collaboration, JHEP 1005 (2010) 032

Geometrical saturation scale (GSS)

- We calculate $\ln(1/x_{GSS})$ and $\ln(Q^2 + M^2)$ for each VM at all the calculated Q^2.
- Dependence is described by a linear fit with slope (1.04 ± 0.07).
- Obtained result reminds of the saturation scale $Q_S^2(x)$, however:
  - This is saturation as seen in the impact-parameter plane.
  - It originates from geometrical fluctuations of hot spots in our model.

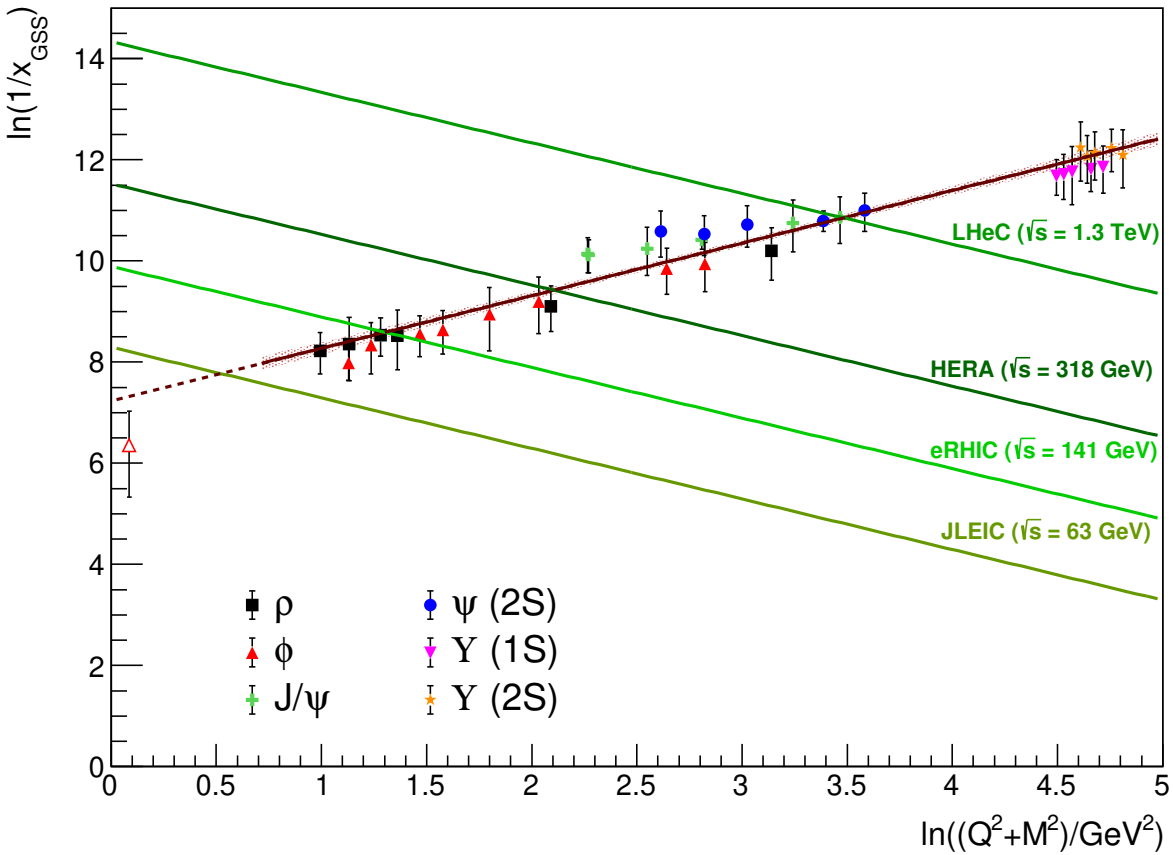

Conclusions - part I

- Succesful implementation of the hot-spot model into the calculation of cross sections for exclusive and dissociative photo and electroproduction of ρ and J/ψ and also ϕ, $\psi(2S)$, $\Upsilon(1S)$ and $\Upsilon(2S)$ mesons *(see in the backup)*.
- All predictions correctly describe the data from HERA and LHC experiments.

Conclusions - part I

- Succesful implementation of the hot-spot model into the calculation of cross sections for exclusive and dissociative photo and electroproduction of ρ and J/ψ and also ϕ, $\psi(2S)$, $\Upsilon(1S)$ and $\Upsilon(2S)$ mesons *(see in the backup)*.
- All predictions correctly describe the data from HERA and LHC experiments.

- Striking behavior of the dissociative cross section dependence on $W_{\gamma p}$
  - Cross section rises at low energies.
  - At a certain energy, available area in the proton is filled $\rightarrow$ hot spots overlap $\rightarrow$ all the possible configurations start to look alike $\rightarrow$ variance decreases.
  - After reaching a maximum at that energy, the cross section starts to decrease.

Conclusions - part II

- We predict energies at which maxima of the dissociative cross section for various vector mesons occur.
- Position of the maximum is directly connected to the vector meson mass and virtuality of the exchanged photon.
- Mass and scale dependence of the position is well described by a linear fit (*see in the backup*).
- We predict a power law behavior in $1/x_{GSS}$ for the geometrical saturation scale.
- This scale is less steeper than the saturation scale given by the GBW model.
- Dissociative maxima seem to be within the reach of existing (LHC) and future (EIC) colliders.

BACKUP SLIDES

Wave functions

- The overlap between the photon and vector meson wave functions:

$$|\Psi^*_{VM}\Psi_{\gamma^*}|_T = \hat{e}_f e \frac{N_C}{\pi z(1-z)} \left[m_f^2 K_0(\epsilon r)\phi_T(r,z) - \left(z^2 + (1-z)^2\right)\epsilon K_1(\epsilon r)\partial_r \phi_T(r,z)\right],$$

$$|\Psi^*_{VM}\Psi_{\gamma^*}|_L = \hat{e}_f e \frac{N_C}{\pi} 2Qz(1-z)K_0(\epsilon r)\left[M_{VM}\phi_L(r,z) + \delta \frac{m_f^2 - \nabla_r^2}{M_{VM}z(1-z)}\phi_L(r,z)\right].$$

$$\epsilon = z(1-z)Q^2 + m_f^2; \qquad r \equiv |\vec{r}|$$

- Scalar part of VM wave function from Boosted Gaussian model:

$$\phi_{T,L}(r,z) = N_{T,L} z(1-z) \exp\left[-\frac{m_f^2 R^2}{8z(1-z)} - \frac{2z(1-z)r^2}{R^2} + \frac{m_f^2 R^2}{2}\right].$$

$$\phi^{2S}_{T,L}(r,z) = \phi_{T,L}(r,z)\left(1 + \alpha_{2S}\left(2 + \frac{m_f^2 R^2}{4z(1-z)} - \frac{4z(1-z)r^2}{R^2} - m_f^2 R^2\right)\right)$$

Skewedness correction

- Takes into account the fact, that there are two x involved in the dipole-target interaction

$$R_g(\lambda_{T,L}) = \frac{2^{2\lambda_{T,L}+3}}{\sqrt{\pi}} \frac{\Gamma\left(\lambda_{T,L}+\frac{5}{2}\right)}{\Gamma(\lambda_{T,L}+4)}, \qquad \lambda_{T,L} \equiv \frac{\partial \ln\left(\mathcal{A}_{T,L}^{\gamma^* p \to VMp}\right)}{\partial \ln\left(\frac{1}{x}\right)}. \tag{1}$$

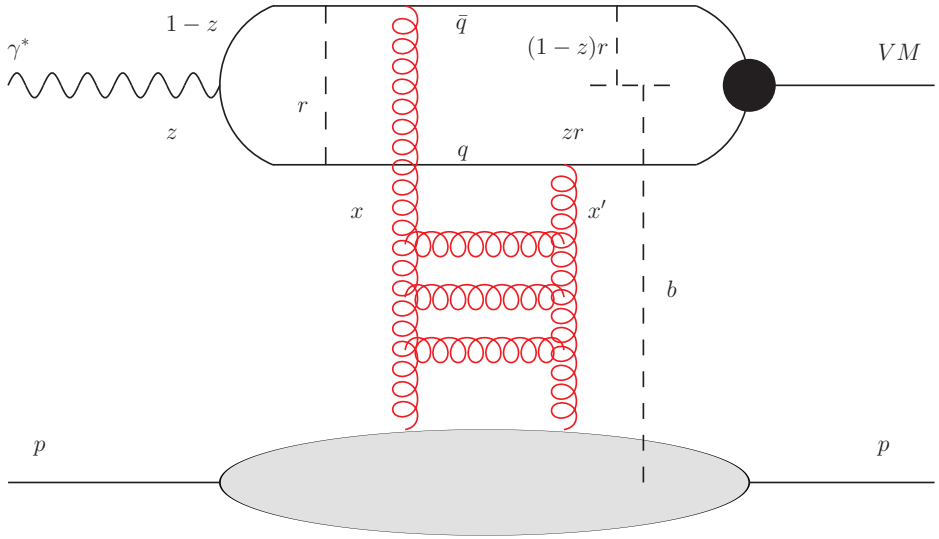

Figure: Schematic picture of vector meson production within the color dipole approach.

Predictions and comparison with data for cross sections of ϕ meson

- Predictions compared to H1 and ZEUS data.
- Decription of the electroproduction data is satisfactory, however not as good as for ρ.
- Again, in photoproduction B_p was changed to $B_p = 8\ \mathrm{GeV}^{-2}$.

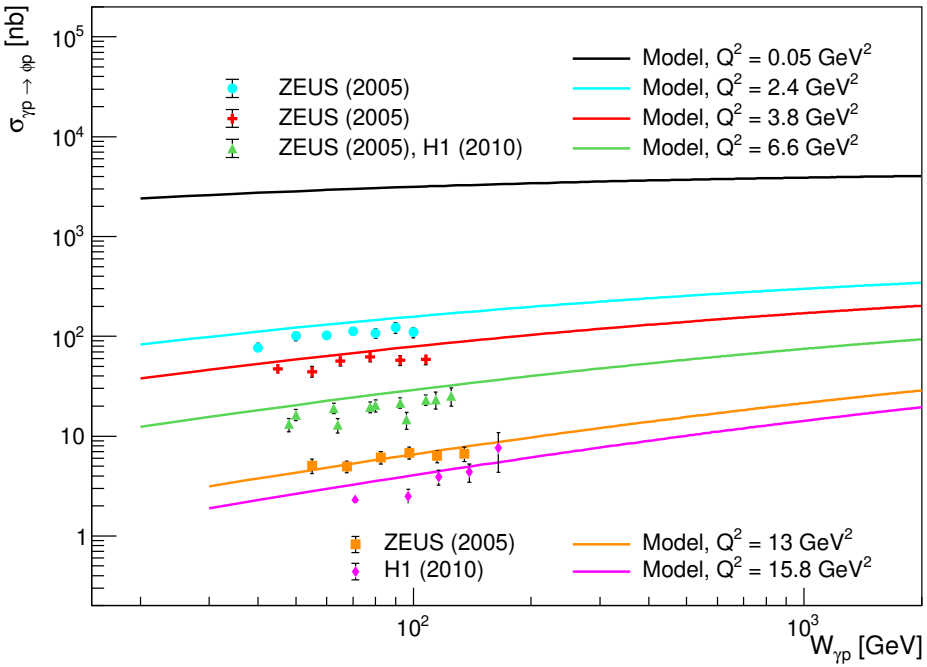

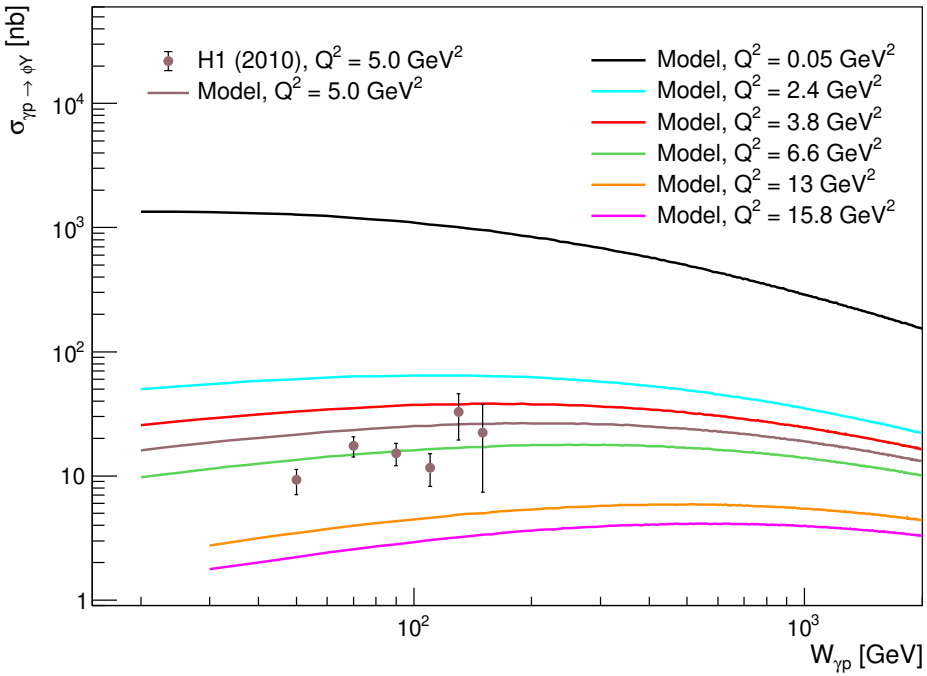

Predictions for cross sections of $\psi(2S)$ meson

- No data are available for cross sections.
- Exclusive $\psi(2S)/J/\psi$ ratios are in fair agreement with the data.

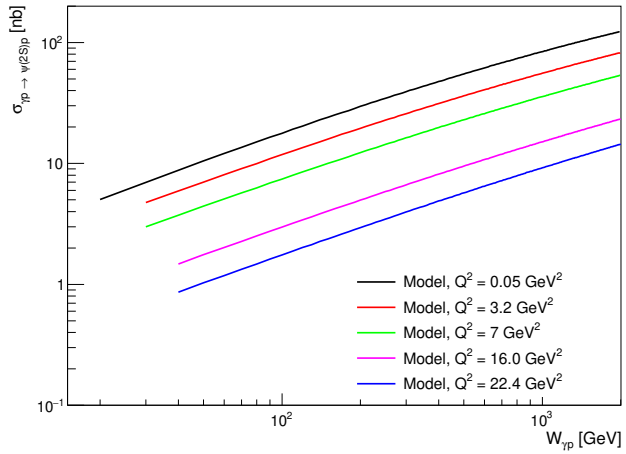

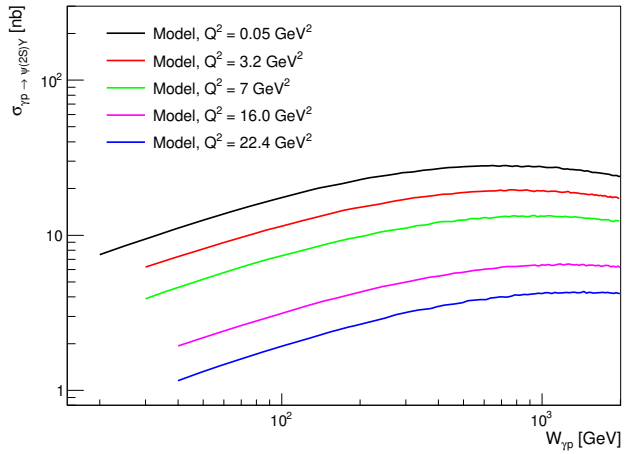

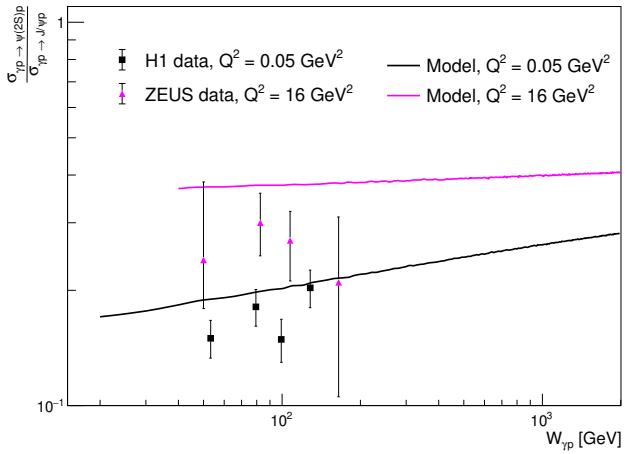

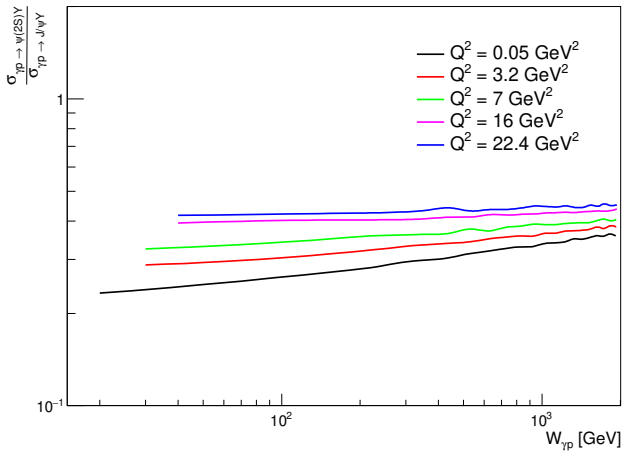

Predictions and comparison with data for cross sections of Υ meson

- Photoproduction predictions compared to H1, ZEUS, CMS and LHCb data.
- Description of the data is reasonable given the large uncertainties.
- No data are available for electroproduction nor for the dissociative process.

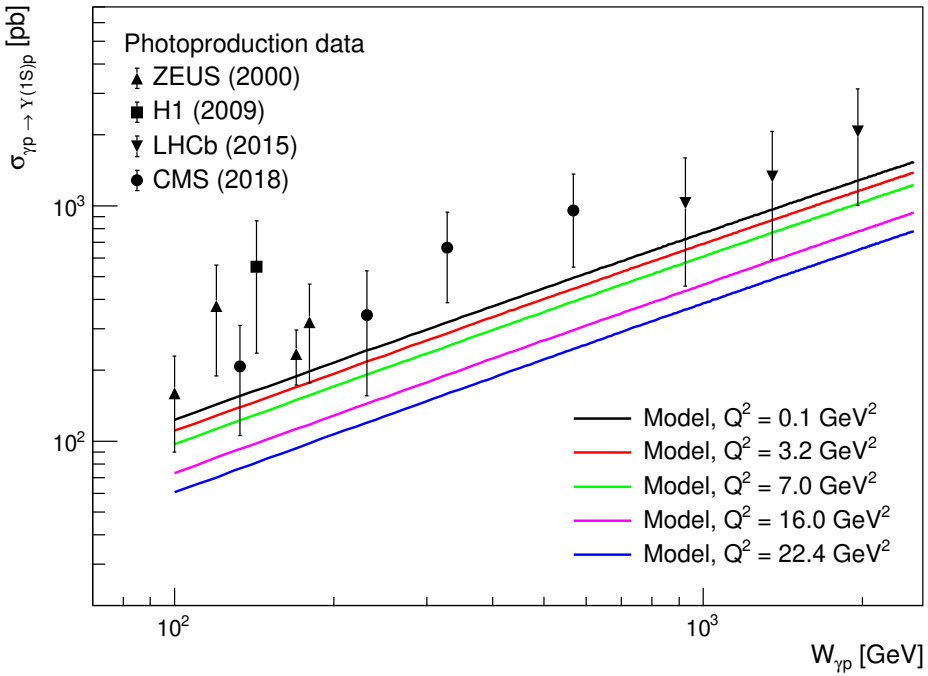

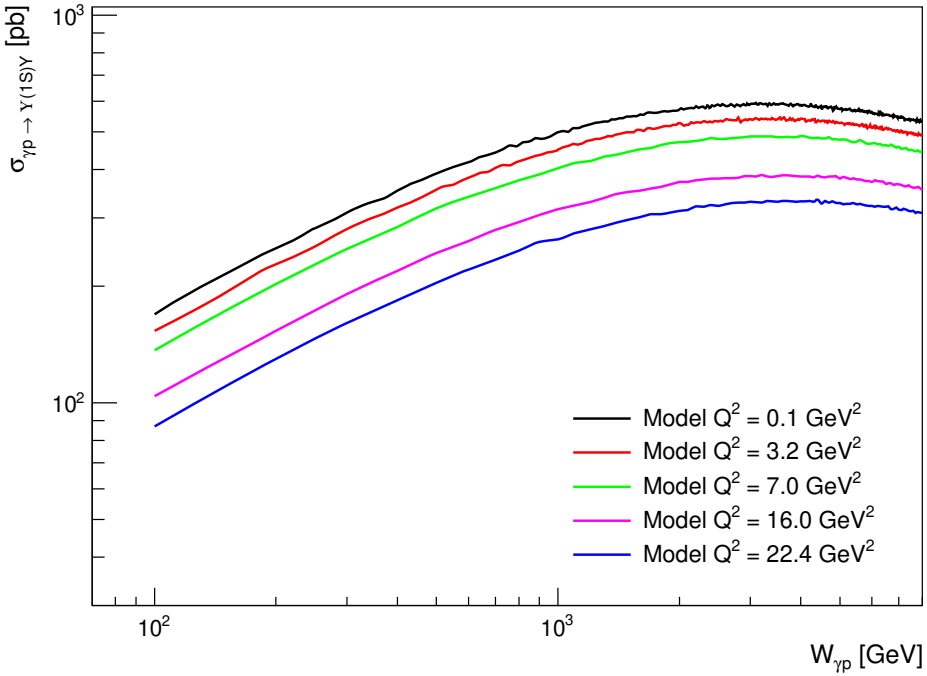

Predictions for cross sections of $\Upsilon(2S)$ meson

- No data are available for cross sections nor for the $\Upsilon(2S)/\Upsilon(1S)$ cross section ratios.

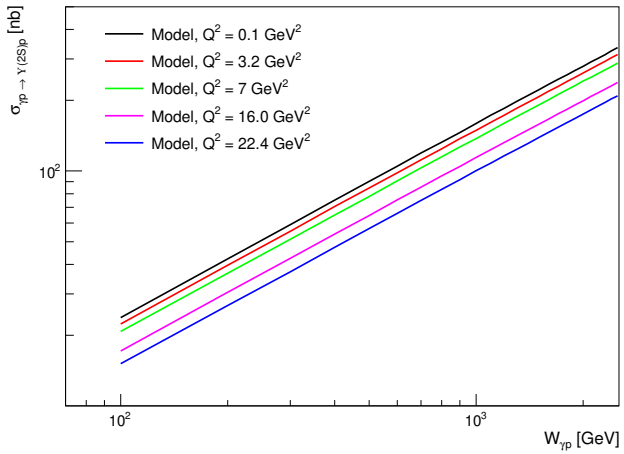

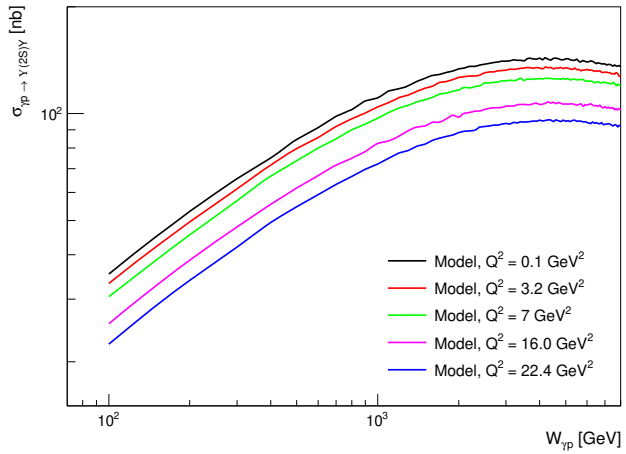

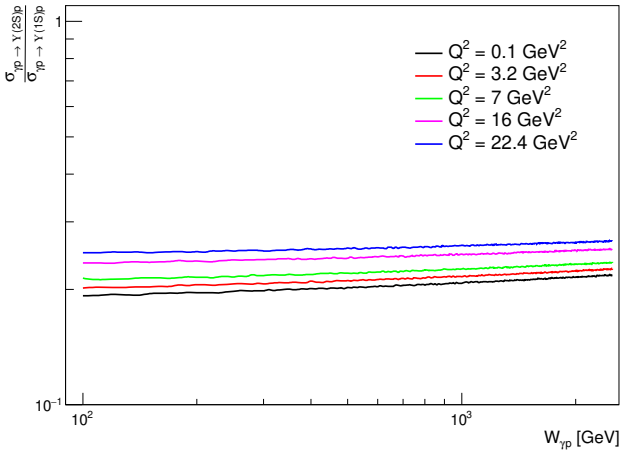

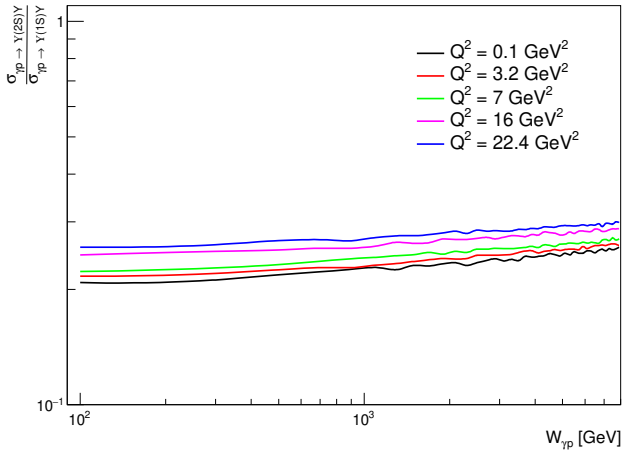

Mass and scale dependence of the position of the dissociative maximum

- We investigate the energy W_{GSS} at which maximum is reached.
- Due to random fluctuations we take 1% of the largest cross section around the maximum at energy value W_{GSS} as an uncertainty interval.
- Maximum is shifted towards higher W_{GSS} with increasing Q^2 and mass M of given vector meson $\rightarrow$ linear fit describes the behavior with a slope $(41 \pm 2)\ \mathrm{GeV}^{-1}$.

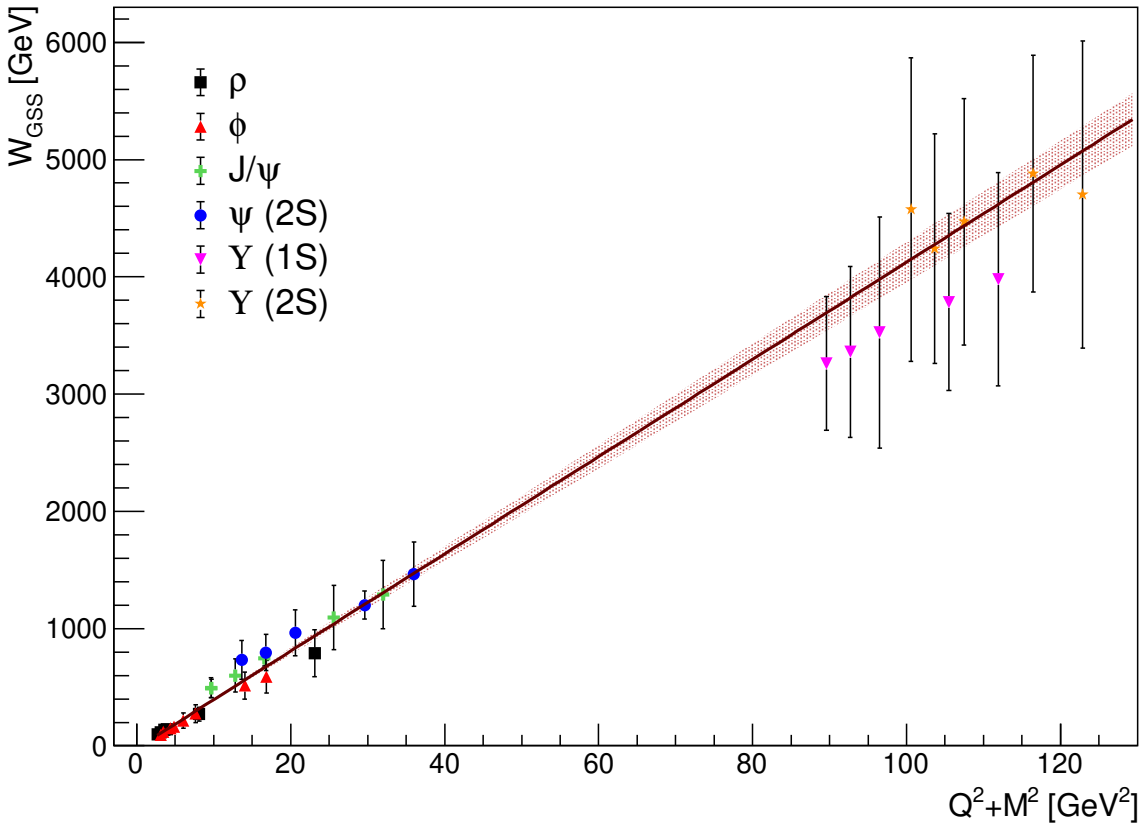

Geometrical vs GBW saturation scale

- Comparison of the geometric saturation scale with the saturation scale obtained from the GBW model:

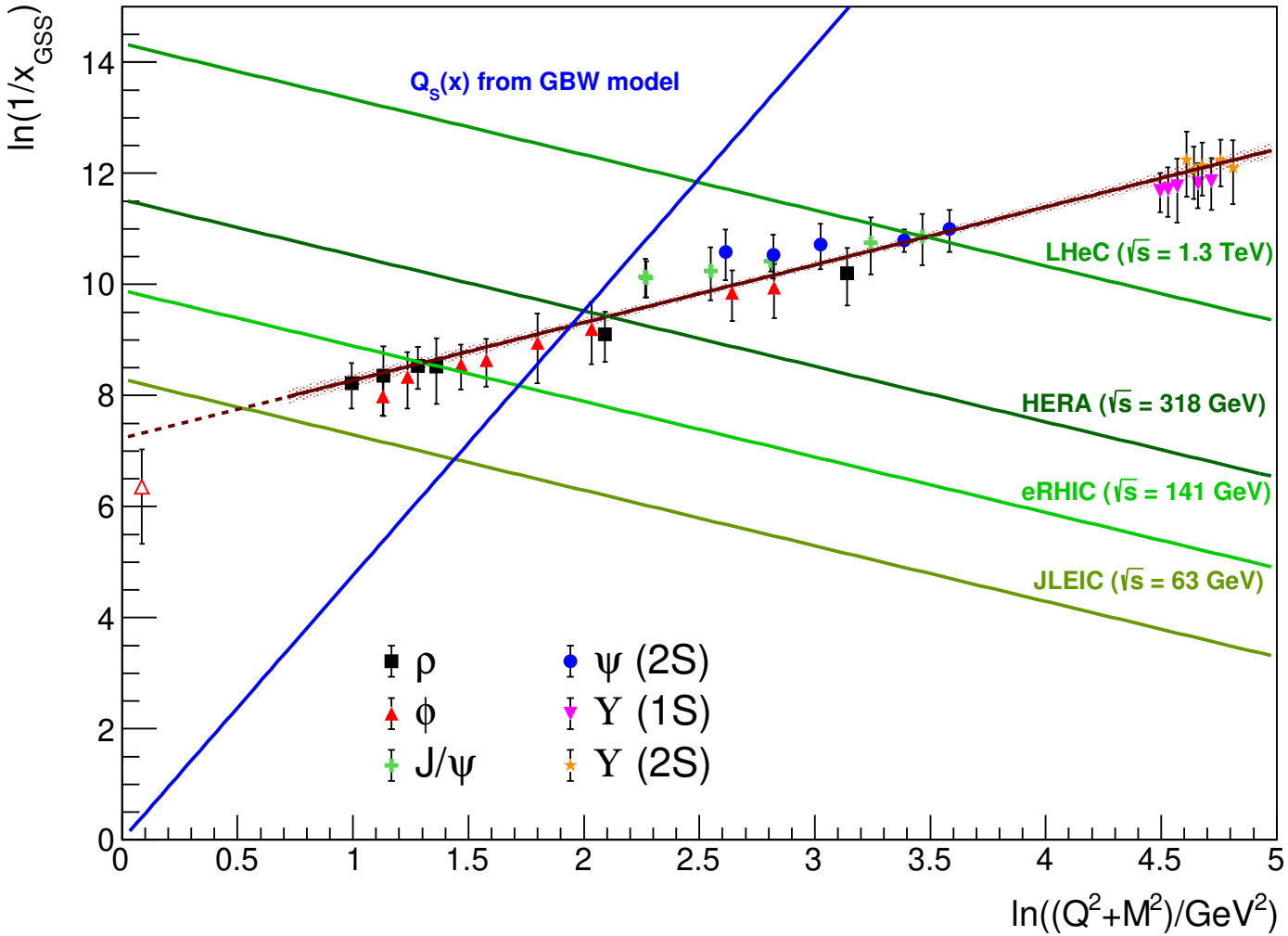

DIS: Structure function $F_2(x, Q^2)$ [6]

- Cross section for $\gamma^* p$ scattering and structure function F_2

$$\sigma_{T,L}^{\gamma^* p} = \sum_f \int \mathrm{d}^2 r \int \mathrm{d}z |\Psi^* \Psi|_{T,L}^f \sigma_{q\bar{q}}(\tilde{x}, r), \qquad F_2(x, Q^2) = \frac{Q^2}{4\pi^2 \alpha}(\sigma_T + \sigma_L).$$

$$\tilde{x} = x\left(1 + \frac{4m_f^2}{Q^2}\right), \qquad Q^2 = 2.7\ \mathrm{GeV}^2$$

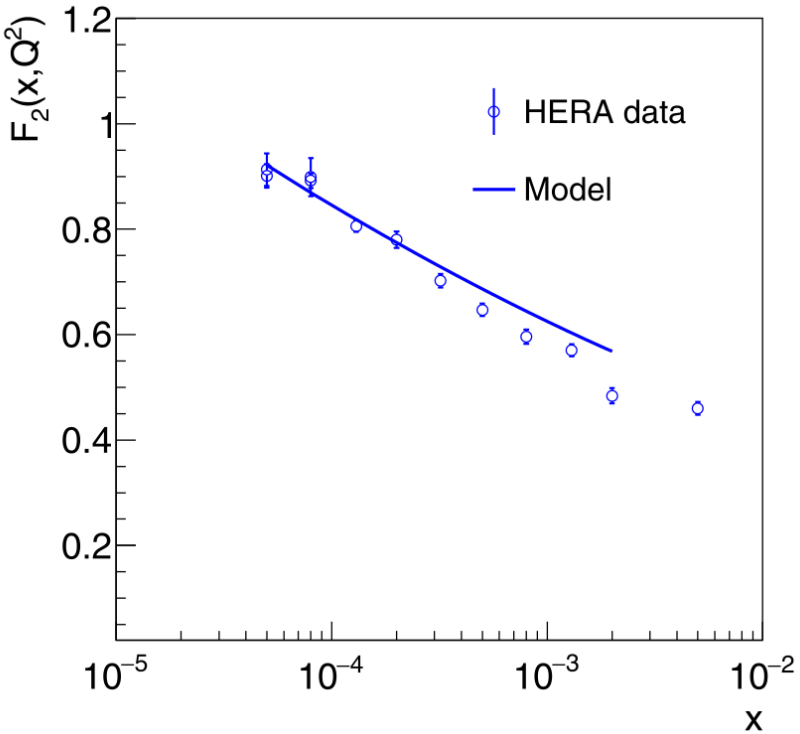

[6] J. Cepila, J. G. Contreras and J. D. Tapia Takaki, Phys.Lett. B766 (2017) 186-191

Exclusive and dissociative $|t|$-distribution of the J/ψ cross section[7]

- Compared with published HERA data.
- Used to tune $T_p(\vec{b})$ parameters.

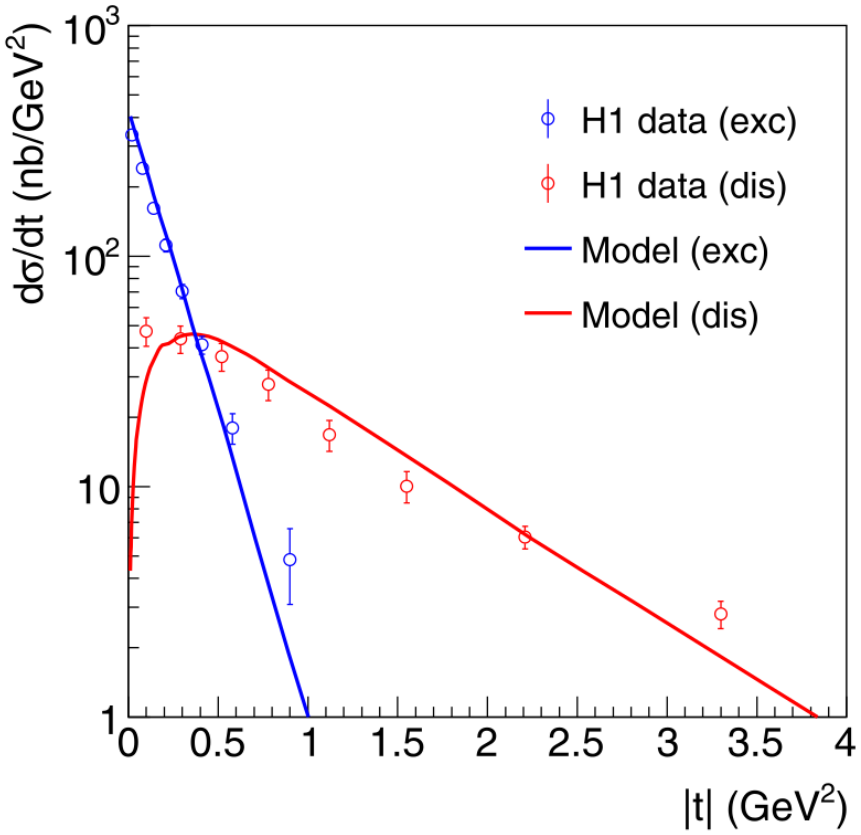

[7] J. Cepila, J. G. Contreras and J. D. Tapia Takaki, Phys.Lett. B766 (2017) 186-191